IEEE Access
Multidisciplinary ⋮ Rapid Review ⋮ Open Access Journal

Received November 15, 2021, accepted December 1, 2021, date of publication December 6, 2021,
date of current version December 17, 2021.

Digital Object Identifier 10.1109/ACCESS.2021.3133287

Research on the Influence of Under-Chassis Equipment Parameters and Distribution on Car Body Vibration of High-Speed Railway Vehicle

BINGSHAO LI, JINSONG ZHOU, DAO GONG, AND TAIWEN YOU
Institute of Rail Transit, Tongji University, Shanghai 201804, China

Corresponding author: Taiwen You (youtaiwen@163.com)

This work was supported by the Fundamental Research Funds for the Central Universities under Grant 22120210558.

ABSTRACT Under-chassis equipment for a high-speed railway vehicle contributes significantly to the vibration response characteristics of the car body. To study the influence pattern of the under-chassis equipment parameters and position distributions on the vibration response of a car body, a rigid-flexible coupling dynamics model of a high-speed railway vehicle is established. The impact of the suspension frequency and mass of the equipment on the vibration of the car body is analyzed. Subsequently, the influence of the equipment placement on the vibration characteristics of the vehicle body is investigated. Furthermore, the study found that the response from a single point cannot represent the vibration performance of the entire vehicle body when adjusting the equipment distribution. To address this challenge, an upper envelope of multiple response points is proposed as an evaluation index. The envelope is applied to study the combined influence of the equipment mass, suspension frequency, and equipment location distribution on the vibration response. The results indicate the effect pattern of equipment suspension frequency, mass, and location arrangement on vehicle body vibration, as well as their combined influence. A suitable parameter and distribution matching relationship is provided by the results to reduce car body vibrations.

INDEX TERMS Railway vehicle, vibration response, hanging equipment, suspension parameters, equipment arrangement.

I. INTRODUCTION

Rapidity and comfort are significant factors for high-speed trains. Moreover, it is an inevitable choice for high-speed trains to be lighter to obtain higher speed, lower energy consumption, and improve the wheel-rail relationship. However, the disadvantages of vehicle lightweighting cannot be ignored. This means that the structural stiffness of the vehicle body is reduced. Consequently, the inherent frequency of the vehicle body can approach the excitation frequency, resulting in a higher probability of resonance and a serious deterioration in passenger comfort [1].

One way to solve this problem is to adjust the relevant parameters or the structure of the vehicle. Zong *et al.* [2]. optimized the second suspension parameters of a railway vehicle using a genetic algorithm. Thus, the impact of resonance on stability was reduced. Dumitriu and Stnic [3]. investigated the effect of primary suspension damping on the vibration level of a body using numerical simulations. Wang *et al.* [4]. introduced the theory of robust optimization to improve the vertical running stability of vehicles. This method considers the influence of noise factors on the results; thus, the optimization results are more robust. Yuewei [5], Yuewei *et al* [6]. developed a vehicle system model containing a vehicle body, a bogie, and a seat. The vertical dynamics of the system were analyzed via numerical simulations. Subsequently, the connection parameters between each subsystem were further optimized. Another approach is to introduce a control system. Molatefi *et al.* [7]. added piezoelectric elements to control the vibration of the car body. Zhou *et al.* [8]. introduced a method to design dynamic dampers using magnetorheological elastic materials to achieve semi-active control of vehicle vibrations. Wang *et al.* [9]. proposed a semi-active damping model based on a sky-hook and linear quadratic regulator control strategy to reduce vehicle body vibrations. Sharma and Lee [10]. established a 28 DOF mathematical model of a railway vehicle and developed a smart semi-active suspension for a vehicle system.

The associate editor coordinating the review of this manuscript and approving it for publication was Jesus Felez.

On the other hand, power dispersion technology is the mainstream technology for high-speed trains, which results in higher traction, flexible grouping, and good speed regulation performance. High-speed trains with power dispersion technology need to install various equipment under the chassis of the car body, such as traction converters, air compressors, and high-voltage boxes. The equipment of a car body is generally suspended under the crossbeams or side beams of the chassis. Because the mass of some pieces of equipment is usually large and some of them generate excitation to the vehicle, the equipment and distribution parameters usually have a large effect on the overall vehicle modal frequency. This effect can change the vibration performance of the vehicle body. Furthermore, the effect is greater for heavy equipment because of the light weight of the body. If the equipment-related factors are not set properly, it will aggravate the oscillation of the car body because of the coupling of the self-vibration frequency of the car body and the equipment. In contrast, a reasonable setting case can have a suppressive effect on the vibration of the car body [11]. Consequently, researching the influence pattern of equipment-related parameters on vehicle body oscillation and using the suppression effect of the equipment for body vibration is a way to improve vehicle body ride comfort. This method is cheaper and more efficient than the two approaches mentioned above; therefore, it has become a hot research topic.

Many researchers have studied the impact of equipment on the vibration of the vehicle body, generally by establishing a rigid-flexible coupling model of the vehicle body. For instance, Sun *et al.* [12]. built a vertical dynamics model of a railway vehicle and explored the effect of static deflection of equipment suspension elements on the ride quality of a vehicle at different speeds. Optimal values of the static deflection were then provided. Sun *et al.* [13]. developed a vehicle dynamics model by Simpack and used two theories of the dynamic vibration absorber method (DVA) and vibration isolation theory for oscillation damping design. The effects of these two methods were compared. Huang *et al.* [14]. verified the established mathematical model of vertical rigid-flexible coupling through field tests and studied the impact of equipment suspension parameters on passenger comfort. Chen *et al.* [15]. considered a vertical mathematical model of a vehicle body containing a single mounted equipment and introduced the analytical target cascade (ATC) method for the multi-objective optimization of suspension parameters. Dumitriu [16] compared a numerical model with equipment and a numerical model without equipment, and analyzed the difference in ride comfort caused entirely by the suspension equipment. Shi *et al.* [17]. established a two-stage vibration isolation system to reduce the oscillation transmission of the equipment. Xiao *et al.* [18]. researched the respective impacts of the auxiliary converter position and suspension parameters on the dynamic characteristics of an urban railway vehicle. However, for most of the studies, the major focus is on the effect of a single equipment suspension parameter (e.g., suspension frequency) on vehicle oscillation. The influence of equipment distribution on vehicle oscillation and the combined effect of equipment positions and parameters have been less studied. In particular, few studies have been conducted on the arrangement of multiple equipment. In practice, the impact of the arrangement of the equipment is a realistic problem to be considered in vehicle design. Currently, the arrangement of equipment relies heavily on the experience. If the matching relationship between the parameters and position is not reasonable, there will be a risk of increasing the vibration of the car body. Therefore, it is meaningful to study the combined effect of equipment mass and suspension frequency on vehicle oscillation under different equipment location distributions. According to the combined effect, a matching relationship can be provided to reduce the vibration, and the ride comfort of the vehicle can be improved.

This study investigates the influence of equipment parameters and distribution on the oscillation transmission characteristics of a railway vehicle body. First, a mathematical model of a complete ready-state vehicle containing several pieces of equipment was developed. The frequency–response function was obtained through numerical calculations using the model. Then, the individual parameters of the equipment were explored for their impact on the oscillation transmission characteristics. The mechanisms underlying the effects of these parameters were further analyzed. Furthermore, the effect of equipment distribution on the vibration behavior of the vehicle was studied. In addition, it was found in the study that a single response point cannot provide a comprehensive vibration evaluation criterion in the study of equipment distribution effects. To address this problem, a multi-point envelope evaluation method is proposed. Based on this approach, the combined influence of the suspension parameters and equipment placement distribution on car body vibration was investigated. Finally, an equipment parameter and distribution matching relationship that can reduce vehicle vibration is proposed.

II. MATHEMATICAL MODEL OF THE VEHICLE WITH MULTIPLE SUSPENDED EQUIPMENT

In this study, a rigid-flexible coupling dynamic model of a high-speed railway vehicle with multiple pieces of under-chassis equipment was established to study the effects of assorted equipment parameters on vehicle body vibration. As illustrated in Figure 1, the model comprises a car body, two bogies, four wheelsets, three principal suspended pieces of equipment, and a suspension system for equipment and bogie. Two rigid modes are owned by the car body, namely, the bounce and pitch modes. To consider the flexibility of the car body, a homogenous free-free Euler-Bernoulli beam with a consistent cross section is introduced as the equivalent model of the car body. The flexible beam was connected to the bogie frames through a secondary suspension system. In addition, owing to the vehicle's low secondary suspension stiffness, the boundary condition of the car body

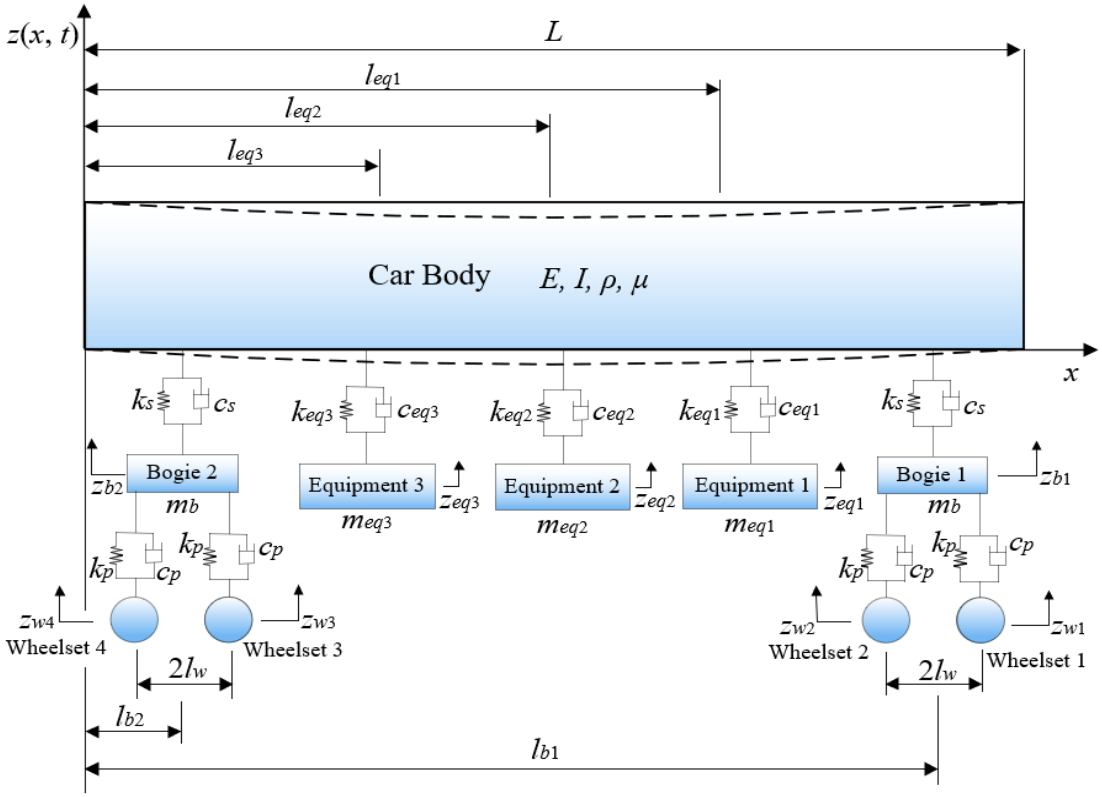

FIGURE 1. Model of the high-speed railway vehicle.

can be free at both ends. The bogie framework is likewise regarded as a rigid body with two levels of freedom, pitch and bounce, sustained on the wheelsets by the primary suspension. It is assumed that the track is rigid and the wheel flange is in close contact with the rails without bounce; that is, the vertical displacement of the wheelset is equal to the vertical irregularity of the track. Notwithstanding the departure from the factual case, this assumption is valid because the rail's natural frequency is much more unusual than the frequency range in this study. The bogies, equipment, and wheelsets were numbered from right to left of the car body.

The parameter representation and coordination definitions of the model are shown in Figure 1. The positive x-axis points to the right, whereas the z-axis has an upward positive direction. The vehicle ran at a consistent speed v along the direction of the x-axis. $z(x,t)$ is the vertical oscillation displacement of the car body, where x is the position coordinate separated from the leftmost end of the entire vehicle, and t is the time variable. z_{b1} and z_{b2} denote the perpendicular displacements of the 1st bogie framework and 2nd bogie framework, respectively. The irregularity excitation of the 1st to 4th wheelsets from the rails is represented by z_{w1} to z_{w4}. Descriptions of the other parameters in Figure 1 are listed in Table 1.

According to relevant theories about structural dynamics [19], the equation of flexible vibration for the car body can be obtained as

$$EI\frac{\partial^4 z(x,t)}{\partial x^4}+\mu I\frac{\partial^5 z(x,t)}{\partial t\partial x^4}+\rho\frac{\partial^2 z(x,t)}{\partial t^2}=P_b+P_{eq} \quad (1)$$

where P_b and P_{eq} represent the forces from the bogies and the suspended facilities, respectively. P_b and P_{eq} can be derived by:

$$\begin{aligned}P_b=&\sum_{i=1}^{2}k_s[z_{bi}-z(l_{bi},t)]\delta(x-l_{bi})\\&+\sum_{i=1}^{2}c_s[\dot{z}_{bi}-\dot{z}(l_{bi},t)]\delta(x-l_{bi}) \quad (2)\\P_{eq}=&\sum_{j=1}^{n}k_{eqj}[z_{eqj}-z(l_{eqj},t)]\delta(x-l_{eqj})+\cdots\\&\cdots+\sum_{j=1}^{n}c_{eqj}[\dot{z}_{eqj}-\dot{z}(l_{eqj},t)]\delta(x-l_{eqj}) \quad (3)\end{aligned}$$

where n is the number of suspended pieces of the equipment. $\delta(\cdot)$ is the Dirac function, indicating the location functions where P_b and P_{eq} take effect. The vibration equations for each bogie and the equipment are as follows:

$$\begin{aligned}m_b\ddot{z}_{bi}=&\,k_s[z(l_{bi},t)-z_{bi}]+c_s[\dot{z}(l_{bi},t)-\dot{z}_{bi}]\\&-k_p(2z_{bi}-z_{w(2i-1)}-z_{w(2i)})\\&-c_p(2\dot{z}_{bi}-\dot{z}_{w(2i-1)}-\dot{z}_{w(2i)})\end{aligned}$$

TABLE 1. Parameters description of the vehicle model.

Parameters for What	Symbol of the Parameters	Description	Parameters for What	Symbol of the Parameters	Description
Car Body	E	The elastic modulus of the car body material	Under-Chassis Equipment	m_{eqj}	Mass of the under-chassis equipment, $j=1,2,...,n$
	I	The moment of inertia of the car body cross section		k_{eqj}	Stiffness of the connector between under-chassis equipment and car body, $j=1,2,...,n$
	μ	Internal damping coefficient of the car body		c_{eqj}	Damping of the connector between under-chassis equipment and car body, $j=1,2,...,n$
	ρ	Mass of per unit length of the car body		z_{eqj}	Vertical vibration displacement of the under-chassis equipment, $j=1,2,...,n$
	L	Whole length of the car body		l_{eqj}	Distance from the center of each equipment to the left end of the car body, $j=1,2,...,n$
	l_b	Half length of bogie centers			
Bogie	m_b	Mass of each bogie	Vehicle Suspension System	k_p	Stiffness of the primary suspension
	l_{bi}	Distance from the bogies to the left end of the car body, $i=1,2$		k_s	Stiffness of the secondary suspension
	l_w	Half length of wheelsets		c_p	Damping of the primary Suspension
	z_{bi}	Vertical vibration displacement of the bogie, $i=1,2$		c_s	Damping of the secondary Suspension

$$i = 1, 2 \tag{4}$$

$$m_{eqj}\ddot{z}_{eqj} = -k_{eqj}[z_{eqj}(t) - z(l_{eqj}, t)] - c_{eqj}[\dot{z}_{eqj}(t) - \dot{z}(l_{eqj}, t)] \quad j = 1, 2, \ldots, n \tag{5}$$

Considering the free vibration of the system, the solution types for Equations (1) and (4) to (5) can be set in the following form:

$$\begin{cases} z(x,t) = \bar{Z}(x)e^{\mathrm{i}\omega t}, \\ z_{bi} = \bar{Z}_{bi}e^{\mathrm{i}\omega t}, \\ z_{eqj} = \bar{Z}_{eqj}e^{\mathrm{i}\omega t} \end{cases} \tag{6}$$

where $\boldsymbol{\omega}$ is the angular frequency, and i is the imaginary unit, $\mathrm{i} = \sqrt{-1}$. In addition, the movement of wheelsets can be written as:

$$z_{wi} = \bar{Z}_{wi}e^{\mathrm{i}\omega t} \tag{7}$$

Substituting Equations (6) and(7) into Equation(1) and Equations (4) to (5) with simplification, Equations (7) to (9) can be deduced, respectively, signifying the vibration of the car body, bogie, and under-chassis equipment:

$$\begin{aligned} &\frac{\partial^4 \bar{Z}(x)}{\partial x^4} - \kappa^4 \bar{Z}(x) \\ &= \frac{1}{EI + \mathrm{i}\omega\mu I} \\ &\quad \times \left\{ \sum_{i=1}^{2} \Lambda_s[\bar{Z}_{bi} - \bar{Z}(l_{bi})]\delta(x - l_{bi}) + \cdots \right. \\ &\quad \left. \cdots + \sum_{j=1}^{n} \Lambda_j[\bar{Z}_{eqj} - \bar{Z}(l_j)]\delta(x - l_j) \right\} \end{aligned} \tag{8}$$

$$\bar{Z}_{bi} = \hat{K}_s\bar{Z}(l_{bi}) + \hat{K}_p(\bar{Z}_{w(2i-1)} + \bar{Z}_{w(2i)}) \tag{9}$$

$$\bar{Z}_{eqj} = \hat{K}_{eqj}\bar{Z}(l_{eqj}) \tag{10}$$

among the equations above, some fresh defined symbols represent the following significations:

$$\kappa^4 = \frac{\rho\omega^2}{EI + \mathrm{i}\omega\mu I} \tag{11}$$

$$\begin{cases} \Lambda_s = k_s + \mathrm{i}\omega c_s, \\ \Lambda_j = k_{eqj} + \mathrm{i}\omega c_{eqj} \end{cases} \tag{12}$$

$$\begin{cases} \hat{K}_p = \dfrac{k_p + \mathrm{i}\omega c_p}{k_s + \mathrm{i}\omega c_s + 2(k_p + \mathrm{i}\omega c_p) - m_b\omega^2}, \\ \hat{K}_s = \dfrac{k_s + \mathrm{i}\omega c_s}{k_s + \mathrm{i}\omega c_s + 2(k_p + \mathrm{i}\omega c_p) - m_b\omega^2}, \\ \hat{K}_j = \dfrac{k_{eqj} + \mathrm{i}\omega c_{eqj}}{k_{eqj} + \mathrm{i}\omega c_{eqj} - m_b\omega^2} \end{cases} \tag{13}$$

Substituting Equations (9) and (10) into Equation(8), $\bar{Z}(x)$ is resolvable by working out the single equation of Equation(8). To facilitate the solution process, Equation(8) can be written as:

$$\frac{\partial^4 \bar{Z}(x)}{\partial x^4} - \kappa^4 \bar{Z}(x) = \frac{f(x)}{EI + \mathrm{i}\omega\mu I} \tag{14}$$

where,

$$f(x) = \sum_{i=1}^{2} \Lambda_s[\bar{Z}_{bi} - \bar{Z}(l_{bi})]\delta(x - l_{bi}) + \sum_{j=1}^{n} \Lambda_j[\bar{Z}_{eqj} - \bar{Z}(l_{eqj})]\delta(x - l_{eqj}) \tag{15}$$

Green's function $G(x, \xi)$ is used to calculate Equation(14) [20]: The response received at one position x by a unit concentrated force acting at another place ξ, $G(x, \xi)$ is the solution for the following equation:

$$\frac{d^4 G(x,\xi)}{dx^4} - \kappa^4 G(x,\xi) = \frac{\delta(x - \xi)}{EI + \mathrm{i}\omega\mu I} \tag{16}$$

Based on the superposition principle [21], the solution of Equation(14) can be written as:

$$\bar{Z}(x) = \int_0^L f(\xi) G(x,\xi) d\xi \tag{17}$$

in accordance with the character of the Dirac function, Equation(14) can be integrated into

$$\bar{Z}(x) = \sum_{i=1}^{2} \Lambda_s[\bar{Z}_{bi} - \bar{Z}(l_{bi})]G(x, l_{bi}) + \cdots + \sum_{j=1}^{n} \Lambda_j[(\hat{K}_j - 1)\bar{Z}(l_{eqj})]G(x, l_j) \tag{18}$$

When x and ξ are equal to l_{bi} and $l_j (i = 1, 2, j = 1, 2, \ldots, n)$, several equations are solved $\bar{Z}(x)$. These equations can be composed of the following matrix form:

$$\boldsymbol{B}\tilde{\boldsymbol{Z}} = \boldsymbol{C} \tag{19}$$

where, (20)–(22), as shown at the bottom of the next page.

Define $\bar{Z}_w = \bar{Z}_{w1}$, $\bar{Z}_{w2} \sim \bar{Z}_{w4}$ can be presented by

$$\begin{cases} \bar{Z}_{w2} = \bar{Z}_w e^{-i\omega\tau_2} \\ \bar{Z}_{w3} = \bar{Z}_w e^{-i\omega\tau_3} \\ \bar{Z}_{w4} = \bar{Z}_w e^{-i\omega\tau_4} \end{cases} \tag{23}$$

where and $\tau_2 \sim \tau_4$ are time delays from the 1st wheelset to 2nd-4th wheelsets. Expressions for $\tau_2 \sim \tau_4$ are:

$$\begin{cases} \tau_2 = 2l_w/v \\ \tau_3 = 2l_b/v \\ \tau_4 = 2(l_w + l_b)/v \end{cases} \tag{24}$$

Substituting Equations (22) and (23) into Equation(21), $\boldsymbol{C}$ can be written as: (25), as shown at the bottom of the next page.

$G(x, \xi)$ in matrices $\boldsymbol{B}$, $\boldsymbol{C}$, and Equation (18) can be obtained by solving Equation (16). $\tilde{\boldsymbol{Z}}$ is obtained by substituting $\boldsymbol{B}$ and $\boldsymbol{C}$ into Equation (19). Therefore, $\bar{\boldsymbol{Z}}(x)$ can be obtained by substituting $G(x, \xi)$ and $\tilde{\boldsymbol{Z}}$.

To obtain $G(x, \xi)$, the Laplace transformation is applied to solve Equation(16) [22]. Because ξ has several certain values, the variable of the Laplace transformation is x, as follows:

$$\hat{G}(s) = \frac{1}{s^4 - \kappa^4}\left[\frac{e^{-s\xi}}{EI + \mathrm{i}\omega\mu I} + s^3 G(0) + s^2 G'(0) + sG''(0) + G'''(0)\right] \tag{26}$$

The inverse transformation of Equation (26) is:

$$G(x,\xi) = \frac{\phi_4(x - \xi)u(x - \xi)}{\kappa^3(EI + \mathrm{i}\mu I\omega)} + G(0)\phi_1(x) + \frac{G'(0)}{\kappa}\phi_2(x) + \cdots + \cdots + \frac{G''(0)}{\kappa^2}\phi_3(x) + \frac{G'''(0)}{\kappa^3}\phi_4(x) \tag{27}$$

where, $u(\cdot)$ is step function and $\boldsymbol{\phi}_k(x)(k = 1, 2, 3, 4)$ are:

$$\begin{cases} \phi_1(x) = \dfrac{1}{2}(\cosh\kappa x + \cos\kappa x) \\ \phi_2(x) = \dfrac{1}{2}(\sinh\kappa x + \sin\kappa x) \\ \phi_3(x) = \dfrac{1}{2}(\cosh\kappa x - \cos\kappa x) \\ \phi_4(x) = \dfrac{1}{2}(\sinh\kappa x - \sin\kappa x) \end{cases} \tag{28}$$

Based on the boundary condition of the vehicle model, there are:

$$\left.\begin{aligned} EI\frac{d^2 G}{dx^2} = 0 \\ EI\frac{d^3 G}{dx^3} = 0 \end{aligned}\right\} x = 0 \text{ or } x = L \tag{29}$$

this means that $G''(0) = G''(L) = 0$ and $G'''(0) = G'''(L) = 0$. Thus, the final two items in Equation (27) can be ignored. To obtain $G(0)$ and $G'(0)$, the second-and third-order derivations of Equation(27) with $x = L$:

$$\begin{cases} G''(L) = \dfrac{\phi_2(L - \xi)}{\kappa(EI + \mathrm{i}\mu I\omega)} + \kappa^2 G(0)\phi_3(L) + \kappa G'(0)\phi_4(L) \\ G'''(L) = \dfrac{\phi_1(L - \xi)}{\kappa(EI + \mathrm{i}\mu I\omega)} + \kappa^3 G(0)\phi_2(L) + \kappa^2 G'(0)\phi_3(L) \end{cases} \tag{30}$$

$G(0)$ and $G'(0)$ can be received by solving Equation (31):

$$\begin{cases} G(0) = \dfrac{1}{\kappa^3(EI + \mathrm{i}\mu I\omega)} \times \dfrac{\phi_4(L)\phi_1(L-\xi) - \phi_2(L-\xi)\phi_3(L)}{\phi_3^2(L) - \phi_4(L)\phi_2(L)} \\ G'(0) = \dfrac{1}{\kappa^2(EI + \mathrm{i}\mu I\omega)} \times \dfrac{\phi_2(L)\phi_2(L-\xi) - \phi_3(L)\phi_1(L-\xi)}{\phi_3^2(L) - \phi_4(L)\phi_2(L)} \end{cases} \tag{31}$$

Substituting $G(0)$ and $G'(0)$ into Equation(27), the Green's function expression for the car body model is

$$\begin{aligned} G(x,\xi) = \frac{1}{\kappa^2(EI + \mathrm{i}\mu\mathrm{I}\omega)}[&\phi_4(x-\xi)u(x-\xi) + \cdots \\ &\phi_1(x)\frac{\phi_4(L)\phi_1(L-\xi) - \phi_2(L-\xi)\phi_3(L)}{\phi_3^2(L) - \phi_4(L)\phi_2(L)} + \cdots \\ &\phi_2(x)\frac{\phi_2(L)\phi_2(L-\xi) - \phi_3(L)\phi_1(L-\xi)}{\phi_3^2(L) - \phi_4(L)\phi_2(L)}] \end{aligned} \tag{32}$$

As a result, the vibration equation of the vehicle model can be solved by substituting $G(x,\xi)$ back into matrices $\boldsymbol{B}$ and $\boldsymbol{C}$ and Equation(18).

III. INFLUENCE OF UNDER-CHASSIS EQUIPMENT PARAMETERS ON FREQUENCY RESPONSE FUNCTION

The frequency response curves at any position on the car body can be calculated using the theoretical derivation described in Section II. Based on the frequency response function, the independent influences of the suspend frequency, mass, and location of the under-chassis equipment are individually analyzed in this section.

In general, the principle of arranging equipment is to place the heaviest equipment in the middle and lighter equipment on the sides to ensure weight balance in the length direction of the car body. In practice, the most heaviest equipment is approximately 5 tons. Considering the vehicle model with three pieces of equipment in Section II, the intermediate equipment has an initial mass of 5 tons, while the other two (equipment 1 and 3) are 1 ton.

When a piece of equipment is suspended elastically under the chassis, parameter f_{eqj} represents the suspension frequency of each piece of equipment. f_{eqj} is determined by the mass and suspension stiffness of equipment m_{eqj} and k_{eqj}:

$$f_{eqj} = \frac{1}{2\pi}\sqrt{\frac{k_{eqj}}{m_{eqj}}} \quad j = 1, 2, \ldots, n \tag{33}$$

The damping of the connector between the under-chassis equipment and car body c_{eqj} can be calculated by

$$c_{eqj} = 2\zeta\sqrt{k_{eqj}m_{eqj}} \tag{34}$$

where ζ is the subsidence proportion of the rubber material used to manufacture the connector between the equipment and chassis. In general, ζ is set to 0.06.

It is initially assumed that the suspension frequency, suspension stiffness, and damping are the same for all three pieces of equipment, that is, $f_{eqj} = f_{eq}$, $k_{eqj} = k_{eq}$, $c_{eqj} = c_{eq}$.

According to the actual situation, the main initial data of the vehicle model are listed in Table 2.

A. INFLUENCE OF SUSPEND FREQUENCY ON RESPONSE OF CAR BODY

Harmonic excitations were applied to the four wheelsets and were used as the input function when calculating the

$$\tilde{\boldsymbol{Z}} = [\bar{Z}(l_{b1}), \bar{Z}(l_{b2}), \bar{Z}(l_{eq1}), \bar{Z}(l_{eq2}), \ldots, \bar{Z}(l_{eqn})]^{\mathrm{T}} \tag{20}$$

$$\boldsymbol{B} = \begin{bmatrix} 1+\Lambda_s(1-\hat{K}_s)G(l_{b1},l_{b1}) & \Lambda_s(1-\hat{K}_s)G(l_{b1},l_{b2}) & \Lambda_1(1-\hat{K}_1)G(l_{t1},l_{eq1}) & \Lambda_2(1-\hat{K}_2)G(l_{t1},l_{eq2}) & \cdots & \Lambda_n(1-\hat{K}_n)G(l_{t1},l_{eqn}) \\ \Lambda_s(1-\hat{K}_s)G(l_{b2},l_{b1}) & 1+\Lambda_s(1-\hat{K}_s)G(l_{b2},l_{b2}) & \Lambda_1(1-\hat{K}_1)G(l_{b2},l_{eq1}) & \Lambda_2(1-\hat{K}_2)G(l_{t2},l_{eq2}) & \cdots & \Lambda_n(1-\hat{K}_n)G(l_{t2},l_{eqn}) \\ \Lambda_s(1-\hat{K}_s)G(l_{eq1},l_{b1}) & \Lambda_s(1-\hat{K}_s)G(l_{eq1},l_{b2}) & 1+\Lambda_1(1-\hat{K}_1)G(l_{eq1},l_{eq1}) & \Lambda_2(1-\hat{K}_2)G(l_{eq1},l_{eq2}) & \cdots & \Lambda_n(1-\hat{K}_n)G(l_{eq1},l_{eqn}) \\ \Lambda_s(1-\hat{K}_s)G(l_{eq2},l_{b1}) & \Lambda_s(1-\hat{K}_s)G(l_{eq2},l_{b2}) & \Lambda_1(1-\hat{K}_1)G(l_{eq2},l_{eq1}) & 1+\Lambda_2(1-\hat{K}_2)G(l_{eq2},l_{eq2}) & \cdots & \Lambda_n(1-\hat{K}_n)G(l_{eq2},l_{eqn}) \\ \vdots & \vdots & \vdots & \vdots & \ddots & \vdots \\ \Lambda_s(1-\hat{K}_s)G(l_{eqn},l_{b1}) & \Lambda_s(1-\hat{K}_s)G(l_{eqn},l_{b2}) & \Lambda_1(1-\hat{K}_1)G(l_{eqn},l_{eq1}) & \Lambda_2(1-\hat{K}_2)G(l_{eqn},l_{eq2}) & \cdots & 1+\Lambda_n(1-\hat{K}_n)G(l_{eqn},l_{eqn}) \end{bmatrix} \tag{21}$$

$$\boldsymbol{C} = \Lambda_s\hat{K}_p \begin{bmatrix} (\bar{Z}_{w1}+\bar{Z}_{w2})G(l_{b1},l_{b1}) + (\bar{Z}_{w3}+\bar{Z}_{w4})G(l_{b1},l_{b2}) \\ (\bar{Z}_{w1}+\bar{Z}_{w2})G(l_{b2},l_{b1}) + (\bar{Z}_{w3}+\bar{Z}_{w4})G(l_{b2},l_{b2}) \\ (\bar{Z}_{w1}+\bar{Z}_{w2})G(l_{eq1},l_{b1}) + (\bar{Z}_{w3}+\bar{Z}_{w4})G(l_{eq1},l_{b2}) \\ (\bar{Z}_{w1}+\bar{Z}_{w2})G(l_{eq2},l_{b1}) + (\bar{Z}_{w3}+\bar{Z}_{w4})G(l_{eq2},l_{b2}) \\ \vdots \\ (\bar{Z}_{w1}+\bar{Z}_{w2})G(l_{eqn},l_{t1}) + (\bar{Z}_{w3}+\bar{Z}_{w4})G(l_{eqn},l_{t2}) \end{bmatrix} \tag{22}$$

$$\boldsymbol{C} = \Lambda_s\hat{K}_p\bar{Z}_w \begin{bmatrix} (1+e^{-i\omega\tau_2})G(l_{b1},l_{b1}) + (e^{-i\omega\tau_3}+e^{-i\omega\tau_4})G(l_{b1},l_{b2}) \\ (1+e^{-i\omega\tau_2})G(l_{b2},l_{b1}) + (e^{-i\omega\tau_3}+e^{-i\omega\tau_4})G(l_{b2},l_{b2}) \\ (1+e^{-i\omega\tau_2})G(l_{eq1},l_{b1}) + (e^{-i\omega\tau_3}+e^{-i\omega\tau_4})G(l_{eq1},l_{b2}) \\ (1+e^{-i\omega\tau_2})G(l_{eq2},l_{b1}) + (e^{-i\omega\tau_3}+e^{-i\omega\tau_4})G(l_{eq2},l_{b2}) \\ \vdots \\ (1+e^{-i\omega\tau_2})G(l_{eqn},l_{t1}) + (e^{-i\omega\tau_3}+e^{-i\omega\tau_4})G(l_{eqn},l_{t2}) \end{bmatrix} \tag{25}$$

TABLE 2. Main initial data of the vehicle model.

Parameters	Initial Value	Parameters	Initial Value
Mass of the car body	30 t	Stiffness of the primary suspension	2000 kN/m
Bending stiffness of the car body	3.96×10^{9} N·m^2	Stiffness of the secondary suspension	260 kN/m
Internal damping coefficient of the car body	0.015	Damping of the primary Suspension	20 kN·(m/s^{-1})
Mass of equipment 1	1 t	Damping of the secondary Suspension	20 kN·(m/s^{-1})
Mass of equipment 2	5 t	Length of the car body	25 m
Mass of equipment 3	1 t	Half of the distance between bogie centers	9 m
Distance from the barycenter of equipment 1 to the left end of the car body	15 m	Half of the distance between wheelsets	1.25 m
Distance from the barycenter of equipment 2 to the left end of the car body	12.5 m	Distance from the bogie 1 to the left end of the car body	21.5 m
Distance from the barycenter of equipment 3 to the left end of the car body	10 m	Distance from the bogie 2 to the left end of the car body	3.5 m
Mass of the bogie 1	2.2 t	Mass of the bogie 2	2.2 t

frequency response of the vehicle body. The displacement response of the vehicle body is determined such that the oscillation transmission characteristics of the vehicle body can be studied.

Figure 2 shows the variation in the displacement frequency response curves of the car body chassis center at different equipment suspend frequencies, f_{eq}, from 2 to 18 Hz. As shown in the black dot-dash line, the conditions under which pieces of equipment are rigidly fixed to the chassis are also illustrated. It can be observed from Figure 2 that when the

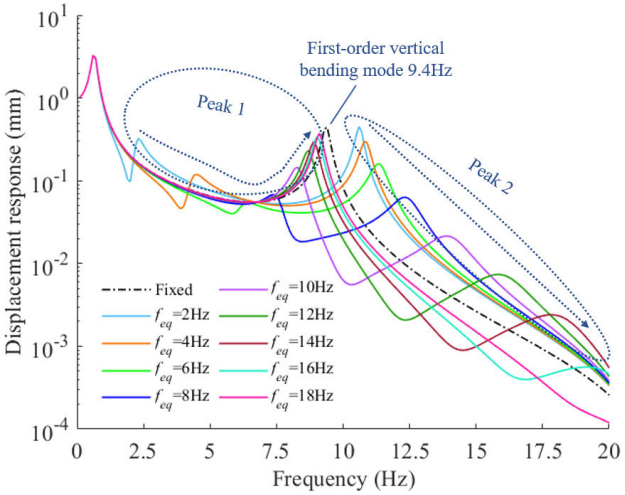

FIGURE 2. Effect of f_{eq} on the frequency displacement response.

pieces of equipment are rigidly fixed, the first-order vertical bending mode frequency of the car body that has the strongest association with vertical vibration is 9.4 Hz. This is consistent with the actual first-order vertical bending frequency of a car body with rigid fixed equipment. When pieces of equipment are elastically suspended, the following phenomenon occurs:

a). The peak frequency matching up to the first-order vertical bending mode is separated into two peaks, with a lower frequency for the first peak and a higher frequency for the second peak. This is because the elasticity of the equipment suspension changes the modal characteristics of the entire system.

b). As f_{eq} increases, both the separated flexible vertical bending mode frequencies increase. This is because the increased stiffness of the equipment suspension elements increases the stiffness of the overall system.

c). When f_{eq} increases, the first peak decreases first, and when f_{eq} rises to 8 Hz, the first peak increases as an alternative. The second peak continued to decrease rapidly with an increase *in* f_{eq}. This is due to the change in f_{eq}. causes a variation in Λ_j and $\hat{K}_j$ in Equation (18), which affects the response.

d). Before 8 Hz, the second peak is greater than the first peak, while after 8 Hz, the second peak is less than the first peak. When f_{eq} increases to a larger value (16–18 Hz), the frequency response curve is similar to that of the rigid fixed equipment because the second peak is not obvious. The further reason is that the suspension stiffness of the equipment is higher for larger suspension frequencies, which is similar to the effect of rigid suspension.

Because a large peak will increase the vibration of the car body and adversely affect the smoothness, either too high or too low af_{eq} is not a good choice. A suspension frequency that can reduce the peak is ideal. In this study, 8–10 Hz was the desired range for the suspended frequency value.

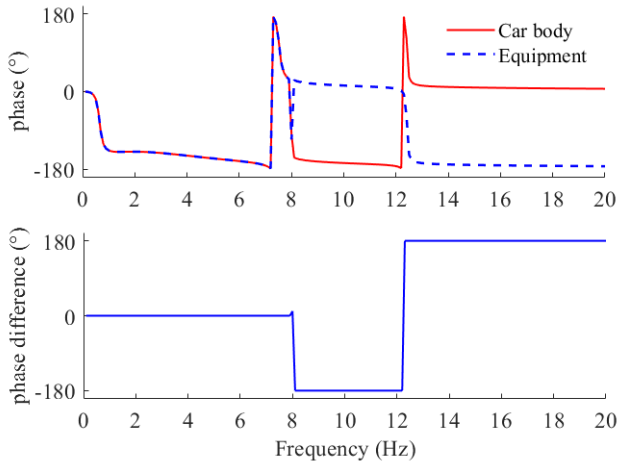

FIGURE 3. Vibration phase at equipment suspension frequency of 8 Hz.

Figure 3 shows the vibration phase of the car body and the equipment. This further illustrates the vibration behavior of the car body and the equipment at 8 Hz. As can be seen from the figure, the vibration phases of the car and the equipment corresponding to the 1st peak are the same. Beginning at 8 Hz of the vibration response frequency, the phase changes abruptly, and an anti-resonance peak appears. This frequency is exactly the equipment suspension frequency, which should be the reason why the elastic suspension of the equipment changes the overall vibration characteristics. Thereafter, the car body and equipment are in opposite phases and are in opposite phases at the 2nd resonance peak. In other words, if the middle of the car body bends upward when vibrating at the 2nd resonance peak, the equipment will move downward.

B. INFLUENCE OF EQUIPMENT MASS ON THE VIBRATION RESPONSE OF THE CAR BODY

In consideration of the type selection and arrangement design of the electrical and mechanical components of the under-chassis equipment, it is necessary to mention the impact of the mass of equipment on the vibration of the entire vehicle. The effect of the mass magnitude on the vehicle vibration is studied here.

Consider the case of equal mass of the two pieces of equipment on both sides (m_{eq1} and m_{eq3}) and gradually increasing the mass of the intermediate equipment (m_{eq2}). Equipment masses on both sides were set to 1 ton, and m_{eq2} was increased from 1 ton to 7 tons in steps of 1. Figure 4 (a) shows the variation in the frequency response curve when all pieces of equipment are rigidly fixed, while Figure 4 (b) shows the elastic suspended situation. With all pieces of equipment having fixed rigidity, both the peak frequency response and its corresponding frequency decrease with increasing mass. This is easy to understand because the modal frequency is equal to the square root of the stiffness divided by the mass. Although the peak becomes lower, the change from increasing mass is still detrimental because it makes the bending flexible mode frequency close to the excitation frequency from the rails. The rigid fixed case with an intermediate equipment weight of 7 tons is also shown as a black dashed curve in Figure 4 (b) for comparison. It can be seen that both peaks of the frequency response in the elastic suspension case are much less than in the rigid fixed case with the same weight.

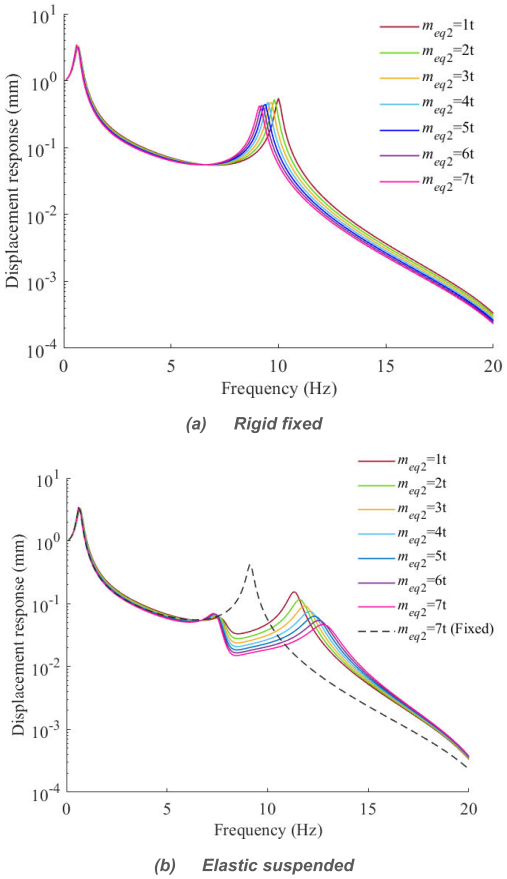

FIGURE 4. Effect of the mass of the intermediate equipment (m_{eq2}) on the frequency displacement response.

In the case of the elastic suspension, the first resonance peak does not change significantly with increasing mass, but the second peak decreases as the mass increases. Meanwhile, the frequency of the bending flexible mode corresponding to the second resonance peak increases with an increase in the equipment mass. The reason for this phenomenon is that when the car body vibrates in anti-phase with the equipment, it can be regarded as part of the mass of the car body being lost. This causes the modal frequency corresponding to the 2nd peak to increase. At the same time, the vibration of the car body is suppressed by the equipment during the anti-phase vibration, and the larger the mass, the more obvious the suppression effect. Therefore, it can be concluded that heavier equipment may effectively reduce the oscillation response of the car body when the equipment is elastically suspended under the chassis at a suitable suspension frequency.

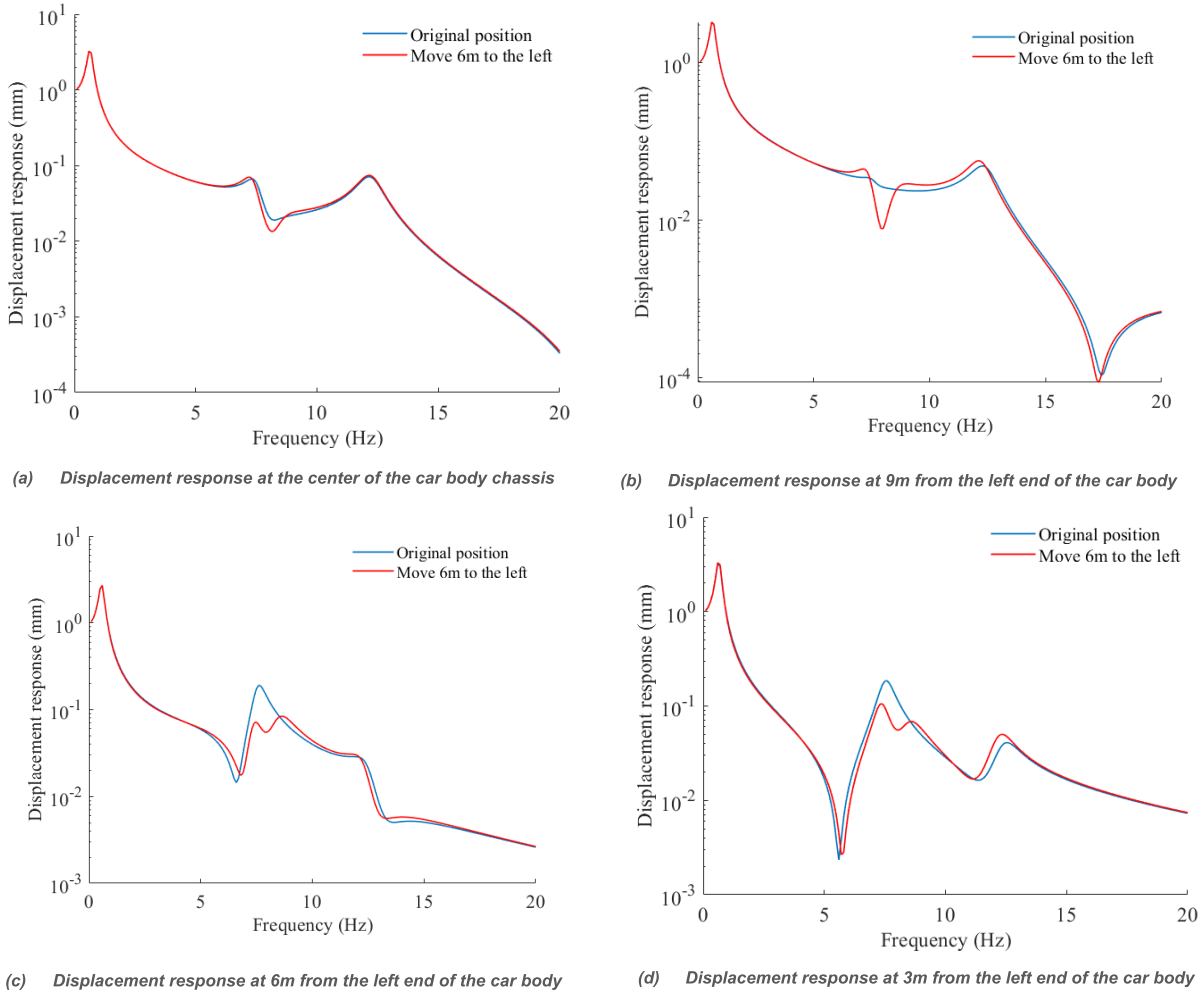

(a) Displacement response at the center of the car body chassis

(b) Displacement response at 9m from the left end of the car body

(c) Displacement response at 6m from the left end of the car body

(d) Displacement response at 3m from the left end of the car body

FIGURE 5. Variation of displacement frequency response curves with the position of equipment 3 at different response points.

IV. MULTI-POINT EVALUATION METHOD OF VEHICLE RESPONESE AND THE EFFECT OF EQUIPMENT DISTRIBUITON ON VIBRATION RESPONSE

Depending on the situation in practice, the position of the equipment may change with different functions, wiring connections, and other requirements, so they may not be at their initial site, or may not even be easily arranged symmetrically. This makes it important to study the impact of different positions of equipment and an asymmetric distribution situation, and it is preferable to find a better distribution scheme.

Four different response points of the car body, the center of the chassis, and the positions of 9 m, 6 m, and 3 m from the left end of the car body, were selected to observe the displacement response curves, as shown in Figure 5 (a) to (d). The displacement frequency response curves of equipment 3 in the original location and in the case of being moved 6 m to the left are illustrated with blue and red curves to study the effect of the change in equipment position. It can be observed that the pattern of change is not the same for the different positions of the response points. However, at 9m from the left extremity of the car, moving the location of the equipment causes both the 1st peak and the 2nd peak to increase. The situation is also different at 6m and 3m from the left end of the vehicle. In the case of 6m from the left end of the car, the 1st peak is reduced by moving the location of the equipment, where the 2nd peak is not significant. At 3m from the left end of the car, the 1st peak decreases and the 2nd peak increases after the movement of the place.

The reason for this problem is probably that when the position distribution is not symmetrical, the first-order vertical bending mode vibration pattern of the car body may no longer be symmetrical about the center. As a result, the response points in the middle of the car body, as in previous studies, may no longer be representative when moving the location or changing the mass of the equipment. This makes it difficult to learn the response variation characteristics of the vehicle body. In addition, it is not possible to find a specific point that always represents the oscillation of the car body as the mass and location of the equipment change. One approach is to select several response points to observe the oscillations. However, there is no information on the variation in positions that are not selected. Considering these challenges, a method that uses the upper envelope of multiple response points to

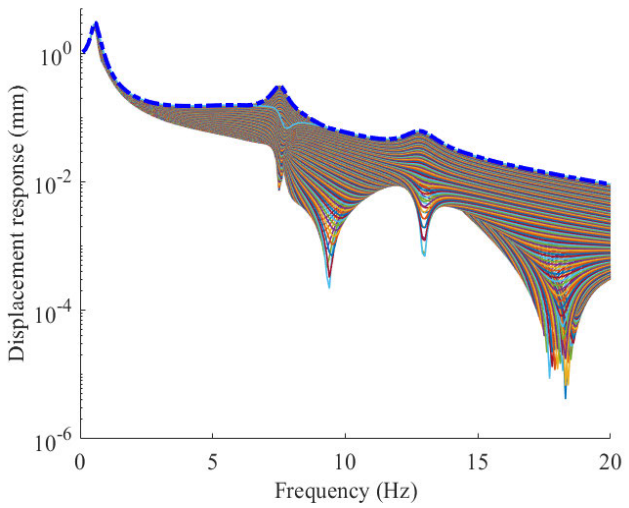

FIGURE 6. Response curves and their upper envelope.

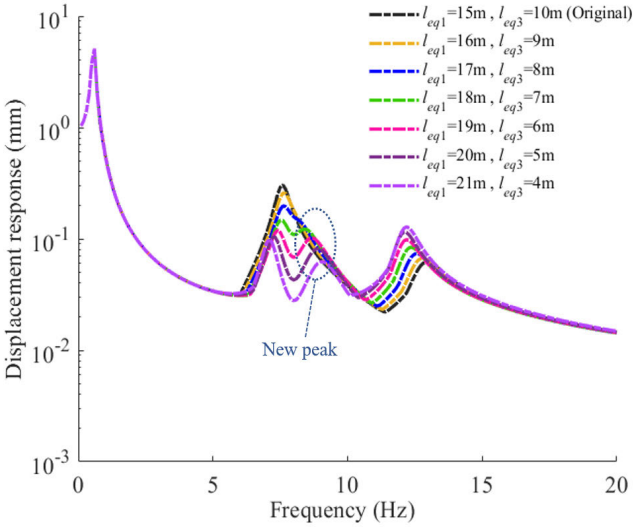

FIGURE 7. Variation of the envelope curve with the position of equipment.

jointly evaluate vehicle body vibration is proposed in this paper.

Response points are picked up in increments of 0.1m from the beginning to the end along the length of the car body. As illustrated in Figure 6, the frequency response curves of all response points are shown, and the blue bold dot-dashed line represents the upper envelope of these response curves. This upper envelope is composed of the maximum response values among all response points corresponding to each frequency. In other words, it is a concatenation of the curves with the highest response in several frequency bands, regardless of which response point these highest response curves come from. This upper envelope curve can characterize the change in the highest response of the body in each frequency band when changing any parameter or distribution of the equipment. Thus, it is appropriate to use the upper envelope curve of multiple response points to study the effect of the equipment position on vehicle vibration.

With all pieces of equipment elastically suspended, equipment 1 and 3 were moved in 1 m steps to both sides to study the variation of displacement frequency response envelope curves for various combinations of positional arrangements.

A case of symmetrical distribution of the equipment is shown in Figure 7, indicating the variation of the displacement frequency response envelope when equipment 1 and 3 are synchronously and equidistantly moved in the direction away from the center of the chassis. It can be seen that as the pieces of equipment on both sides move away from the center, the first peak gradually decreases and a new peak emerges nearly behind it. The new peak is progressively more obvious, but always lower than the first peak. Meanwhile, the second peak rises gradually as the pieces of equipment move away.

Figure 8 (a), (b), and (c) show the variations in the envelope curves with the position of equipment 3 when the locations of equipment 1 are respectively 17m, 19m and 21m, in order to determine the impact of the asymmetric distribution of equipment. It can be found that regardless of the asymmetry, as long as there is a piece of equipment far away from the center of the chassis, there will be a pattern of the first peak reduction and the second peak rising. In addition, the more asymmetrical the two pieces of equipment, the wider the gap between the first peak and the new peak. According to Equations (18) and (32), the basic reason for the above-mentioned pattern of the effect of position can be understood. The variation in the equipment position $\boldsymbol{\xi}$ makes $\boldsymbol{\phi}_1(x) - \boldsymbol{\phi}_4(x)$ changes accordingly. As a result, this leads to a variation in the response $G(x, \xi)$ at each point of the car body.

Figure 9 (a) and (b) illustrate the variation of the first and second peaks in the envelope curves for all possible combinations of different positions. The range of the envelope curve peaks for various location combinations of the equipment can be estimated from Figure 9. It can also be seen that the first peak in the envelope curve decreases as the two pieces of equipment move away from the center of the vehicle, while the second peak increases as the equipment moves. For a compromise, when designing the location of the equipment arrangement, it is necessary to consider that the pieces of equipment on both sides cannot be too far from the center or too close to the center.

V. STUDY OF THE COMPOSITE IMPACT OF EQUIPMENT SUSPENSION PARAMETERS AND DISTRIBUTION ON VIBRATION RESPONSE

According to the study on the influence of mass and suspend frequency parameters of under-chassis equipment, the arrangement of the equipment can be designed in conjunction with mass and suspend frequency parameters to improve the vibration resistance of the car body.

Because the influence of the mass of the intermediate equipment on the oscillation control has already been confirmed, the study of the mass influence mainly considers the various masses of the pieces of equipment on both sides, including the case of balanced and unbalanced distribution of the equipment mass on both sides. Equipment 1 and

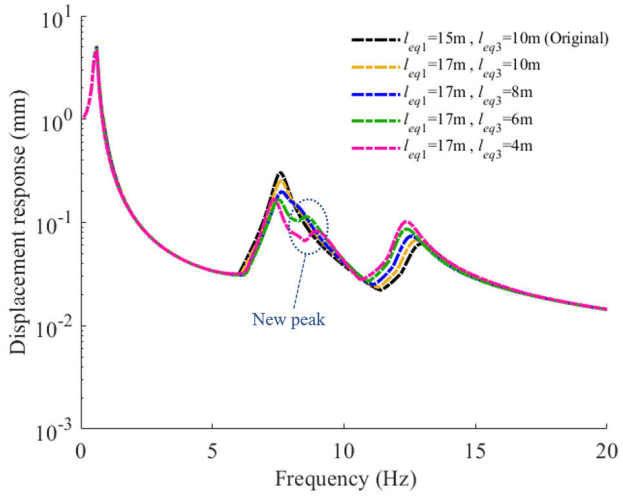

(a) Equipment 1 at 17m

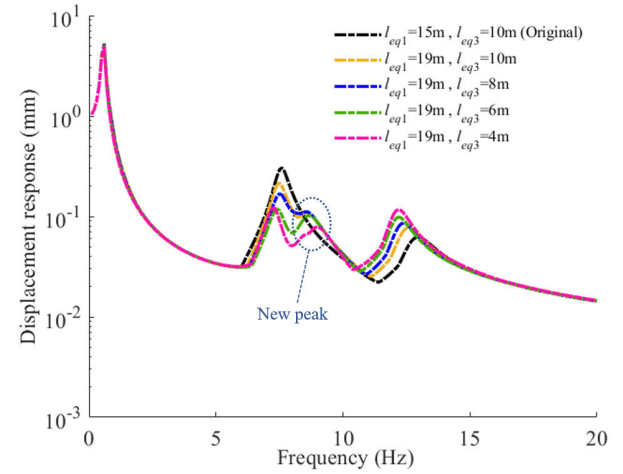

(b) Equipment 1 at 19m

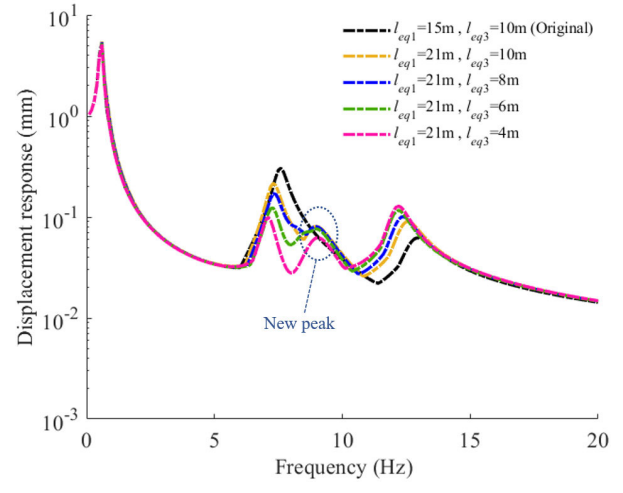

(c) Equipment 1 at 21m

FIGURE 8. **Variation of the envelope curve with the position of equipment 3.**

equipment 3 are respectively varied from 0.5 tons to 3 tons in steps of 0.5 tons. To facilitate the representation of the results of this study, various combined mass configurations

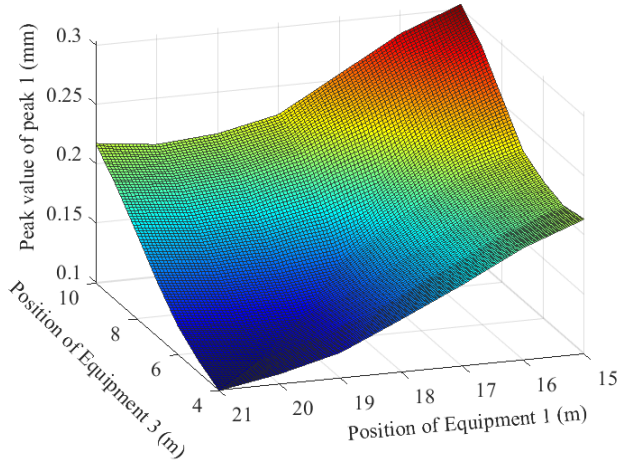

(a) Variation of The first peak

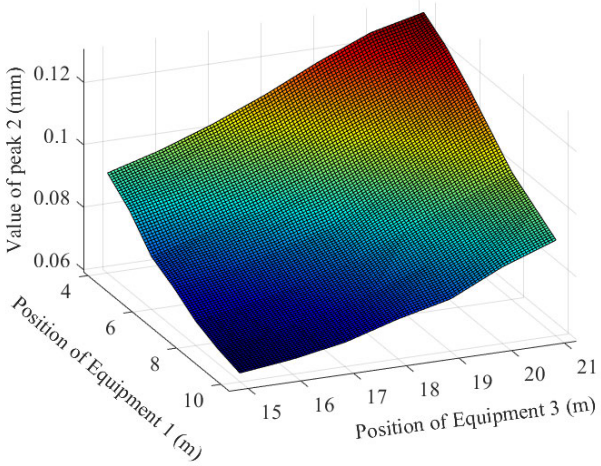

(b) Variation of The second peak

FIGURE 9. **Variation of envelope peaks.**

are defined for a total of 36 cases. Cases 1 to 6 indicate that equipment 3 is 0.5 tons and equipment 1 changes from 0.5 tons to 3 tons, cases 7 to 12 indicate that equipment 3 is 1 ton and equipment 1 changes from 0.5 tons to 3 tons, and so on.

Variations in the first and second peaks for different configurations of equipment masses when the pieces of equipment on both sides are moved synchronously in equal steps of 1m are shown in Figure 10. It can be observed from the figure that for the first peak, the farther equipment 1 and 3 are from the center of the chassis for the same mass configuration, the lower the first peak. When pieces of equipment on both sides are located closer to the center of the chassis, the first peak increases with an increase in the mass of the equipment. However, as the distance increases further, the magnitude of the increase slows down. When the distance is sufficiently large, the first peak decreases with the increase in mass. An increase in the total mass or an increase in the mass of equipment 1 will lead to this result.

For the second peak, the peak value for the same mass configuration shows an increasing trend with increasing distance

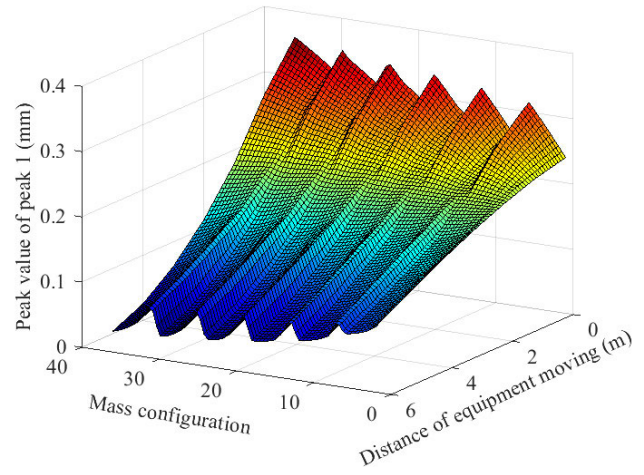

(a) Variation of The first peak

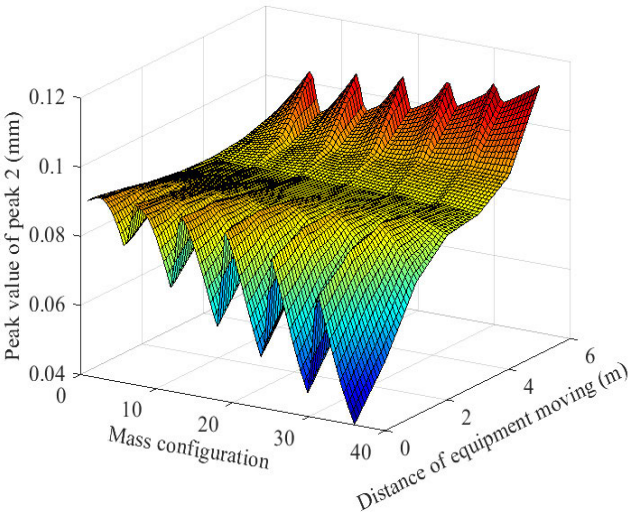

(b) Variation of The second peak

FIGURE 10. Effect of equipment mass and location on vibration response.

of the equipment from the center of the chassis. With a close distance between the flank two pieces of equipment and the center of the chassis, an increase in the total mass or just the mass of equipment 1 causes a subsequent decrease in the second peak. This trend becomes progressively more pronounced as the total mass increases. Conversely, the decrement slows down as the distance increases. When the distance reaches a point, the 2nd peak turns to raise as the mass increases.

The slice diagram in Figure 11 indicates the combined correlation between the different suspension frequencies and the placement distribution of the equipment, as well as the mass configuration. This demonstrates that only lower suspension frequencies (approximately 7 Hz) can reduce the first peak when the two pieces of equipment are placed closer to the center of the chassis. This effect diminishes as the total mass increases. The suspension frequency range that causes the 2nd peak to be effectively reduced is 8.5 to 10 Hz, and as the total mass increases, this effect becomes stronger and the range expands to 8 to 10 Hz. As the flank two pieces of equipment get farther from the center of the chassis, the upper limit of the suspension frequency range that can reduce the 1st peak increases. The heavier the mass, the higher the upper frequency limit. For the second peak, when the pieces of equipment on both sides move far away from the chassis center, the function of the original suspension frequency range to the reduction of the peak is diminished. After the distance reaches 3 m, the suspension frequency range that can reduce the second peak increases progressively. When the pieces of equipment on both sides are moved to 6m from the center of the chassis, a suspension frequency range of 9–12 Hz can effectively reduce the second peak. Based on Equation (18), the root cause of the above pattern can be understood. The equipment position changes $G(x, \xi)$, and the equipment suspension frequency and mass change, Λ_j and $\hat{K}_j$. These changes result in variations in the vehicle response $\bar{Z}(x)$ and create such a matching relationship. The information in this matching relationship can be used as a reference for the influence of the magnitude of the vibration response in the design of the equipment arrangement. The equipment suspension frequencies can be designed based on the equipment location and mass distribution.

VI. CONCLUSION

In this study, a multi-equipment mathematical model of a railway vehicle was developed. With the application of this model, the vehicle vibration response was calculated under various suspension frequencies, masses, and location distributions. The combined impact of these factors on car body vibrations was studied. A new method for synthesizing the upper envelope from multiple response points to evaluate the oscillation performance of the entire car body was proposed. The analysis of the computational results provided the following conclusions.

a). Equipment with an elastic suspension separates the response peaks into two peaks corresponding to the first-order vertical bending mode of the vehicle body. Both are lower than the peaks caused by the first-order vertical bending mode under the original rigid suspension. As the suspension frequency increases, the first peak diminishes and then increases, while the second peak continues to decrease. The suggested suspension frequency range is 8–10 Hz. Because the car body at the 2nd resonance peak is in the opposite phase to the equipment vibration, the increase in the intermediate equipment mass has a beneficial effect on reducing the second peak.

b). In the research of the effect on the vibration response characteristics of the whole vehicle by the variation of equipment distribution, the commonly used method of selecting a single response point to view the response cannot represent the oscillation variation of the whole body. For this reason, a method for calculating the upper envelope of multiple response points to consider the oscillation response of the entire vehicle body is proposed. This approach allows the consideration of the vibration response at all places,

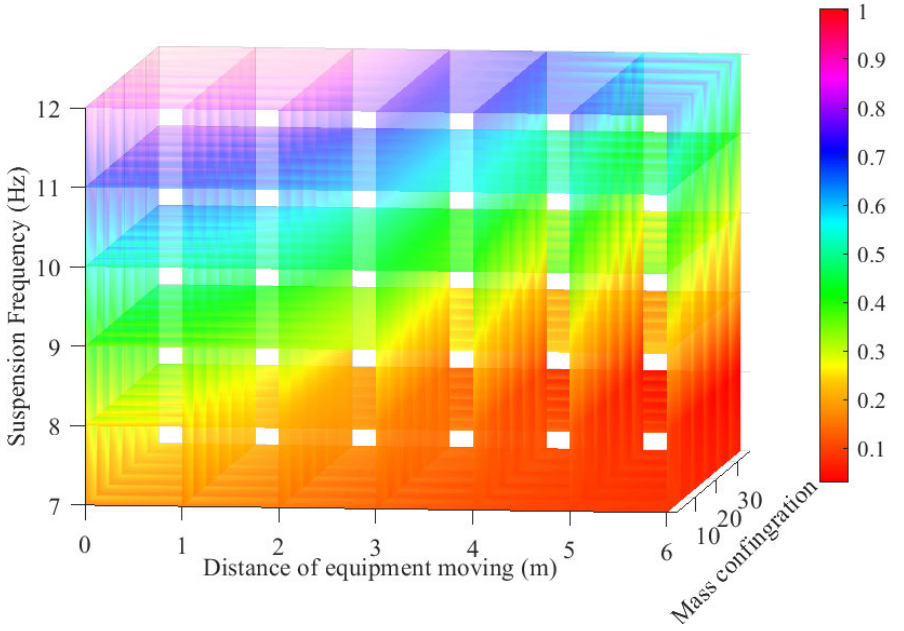

(a) Variation of The first peak

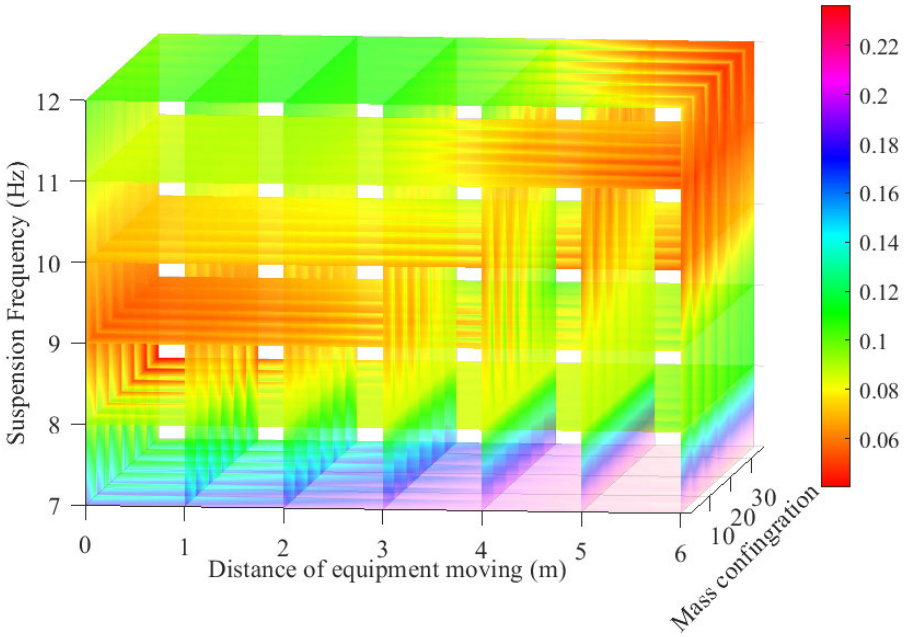

(b) Variation of The second peak

FIGURE 11. Matching relationship between equipment mass, location and suspension frequency.

avoiding the problem of different variation patterns at different response points and uncertain variations at unpicked positions. With the flank pieces of equipment moving away from the center of the vehicle, the 1st peak of the envelope curve decreases, while the 2nd peak increases.

c). With varying mass and location distributions, when the two pieces of equipment on both sides are close to the center of the car chassis, the first peak increases and the second peak decreases as the total mass of the equipment increases. While the pieces of equipment on both sides move away from the center of the chassis, the situation turns to a decrease in the first peak and an increase in the second peak with the increase in mass.

d). A matching relationship between the equipment distribution and the parameters is proposed. As the pieces of equipment on both sides move away from the center, the suspension frequency range that can effectively reduce the first peak is expanded from approximately 7 Hz to 10 Hz.

The range is further expanded with the distance from the center. For the latter peak, a suspension frequency of 8.5–10 Hz can diminish the peak when the pieces of equipment are close to the center of the car chassis. This range expands to 8–10 Hz as the mass of the equipment increases. When the two pieces of equipment are far from the center of the chassis, the suspension frequency range of 9–12 Hz can reduce the peak. This matching relationship can be used as a basis for designing and arranging vehicle chassis equipment to reduce vibrations.

REFERENCES

[1] *Vibration and Control on Railway Vehicles*, Fudan Univ., Shanghai, China, 2019.
[2] C. Zong, D. Chen, Y. Zhou, and G. Shen, "Parameter optimal design of railway vehicle based on genetic algorithm," *Electr. Drive Locomotives*, vol. 263, no. 4, pp. 33–36, 2018.
[3] M. Dumitriu and D. I. Stănică, "Influence of the primary suspension damping on the ride comfort in the railway vehicles," *Mater. Sci. Forum*, vol. 957, pp. 53–62, Jun. 2019.
[4] P. Wang, Y. Yang, B. Yi, W. Zeng, and T. Wang, "Robust optimization of high-speed rail vehicle suspension parameters based on vertical running stability," *J. Mech. Eng.*, vol. 40, no. 6, pp. 583–593, 2019.
[5] Y. Yu, "Vertical coupled vibration mechanism of bogie-body-seat system and joint optimization of suspension parameters for high-speed train," *J. Mech. Eng.*, vol. 54, no. 8, p. 57, 2018.
[6] Y. U. Yuewei, C. Zhou, and L. Zhao, "Vertical dynamic model and analysis of bogie-body-seat coupling system," *J. Railway Sci. Eng.*, vol. 15, no. 1, pp. 196–205, 2018.
[7] H. Molatefi, P. Ayoubi, and H. Mozafari, "Active vibration control of a railway vehicle carbody using piezoelectric elements," *J. Mech. Eng.*, vol. 30, p. 972, Jun. 2017.
[8] W. Zhou, Y. Wen, H. Shang, Z. Zong, and L. Guo, "A study on vibration reduction characteristics of semi-active magnetorheological vibration absorbers for vehicle bodies," *J. Vib. Shock*, vol. 37, no. 16, pp. 124–134, 2018.
[9] Q. Wang, J. Zeng, Y. Wu, and B. Zhu, "Study on semi-active suspension applied on carbody underneath suspended system of high-speed railway vehicle," *J. Vib. Control*, vol. 26, nos. 9–10, pp. 671–679, May 2020.
[10] S. K. Sharma and J. Lee, "Design and development of smart semi active suspension for nonlinear rail vehicle vibration reduction," *Int. J. Struct. Stability Dyn.*, vol. 20, no. 1, 2020, Art. no. 2050120.
[11] D. Gong, J.-S. Zhou, and W.-J. Sun, "On the resonant vibration of a flexible railway car body and its suppression with a dynamic vibration absorber," *J. Vib. Control*, vol. 19, no. 5, pp. 649–657, Apr. 2013.
[12] W. Sun, D. Gong, J. Zhou, and Y. Zhao, "Influences of suspended equipment under car body on high-speed train ride quality," *Proc. Eng.*, vol. 16, pp. 812–817, Jan. 2011.
[13] Y. Sun, D. Gong, and J. Zhou, "Study on vibration reduction design of suspended equipment of high speed railway vehicles," *J. Phys., Conf. Ser.*, vol. 744, Sep. 2016, Art. no. 012212.
[14] C. Huang, J. Zeng, G. Luo, and H. Shi, "Numerical and experimental studies on the car body flexible vibration reduction due to the effect of car body-mounted equipment," *Proc. Inst. Mech. Eng. F, J. Rail Rapid Transit*, vol. 232, no. 1, pp. 103–120, Jan. 2018.
[15] J. Chen, Y. Wu, L. Zhang, X. He, and S. Dong, "Dynamic optimization design of the suspension parameters of car body-mounted equipment via analytical target cascading," *J. Mech. Sci. Technol.*, vol. 34, no. 5, pp. 1957–1969, May 2020.
[16] M. Dumitriu, "Numerical study on the influence of suspended equipments on the ride comfort in high speed railway vehicles," *Sci. Iranica*, vol. 27, no. 4, pp. 1897–1915, 2020.
[17] H. Shi, R. Luo, P. Wu, J. Zeng, and J. Guo, "Influence of equipment excitation on flexible carbody vibration of EMU," *J. Mod. Transp.*, vol. 22, no. 4, pp. 195–205, Dec. 2014.
[18] X. Qian, L. Yanming, and L. Zhixiang, "Influence of suspension position and suspension parameters of vehicle equipment on the vehicle systems," *Noise Vib. Control*, vol. 41, no. 3, pp. 120–126, 2021.
[19] X.-F. Li, "A unified approach for analyzing static and dynamic behaviors of functionally graded Timoshenko and Euler–Bernoulli beams," *J. Sound Vib.*, vol. 318, nos. 4–5, pp. 1210–1229, Dec. 2008.
[20] G. Failla and A. Santini, "On Euler–Bernoulli discontinuous beam solutions via uniform-beam Green's functions," *Int. J. Solids Struct.*, vol. 44, nos. 22–23, pp. 7666–7687, Nov. 2007.
[21] N. Ackermann, "A nonlinear superposition principle and multibump solutions of periodic Schrödinger equations," *J. Funct. Anal.*, vol. 234, no. 2, pp. 277–320, May 2006.
[22] G. Doetsch and L. Debnath, "Introduction to the theory and application of the Laplace transformation," *IEEE Trans. Syst., Man, Cybern.*, vol. SMCB-7, no. 8, pp. 631–632, Aug. 1977.

BINGSHAO LI was born in Tangshan, Hebei, China, in 1997. He received the bachelor's degree in vehicle engineering from Lanzhou Jiaotong University, Gansu, China, in 2019. He is currently pursuing the master's degree in vehicle application engineering with Tongji University, Shanghai, China. His research interests include railway vehicles structural dynamics and system dynamics.

JINSONG ZHOU is currently a Professor at the Institute of Rail and Transit, Tongji University. He has been researching railway vehicle dynamics, modal parameter testing, and control of the vibration and sound of railway vehicles.

DAO GONG is currently an Associate Professor at the Institute of Rail and Transit, Tongji University. He has been researching railway vehicle dynamics, modal parameter testing, and control of the vibration and sound of railway vehicles.

TAIWEN YOU was born in Baiyin, Gansu, China, in 1992. He is currently pursuing the Ph.D. degree in vehicle application engineering with Tongji University, Shanghai, China. His main research interests include structural vibration control and vehicle dynamics.